ORIGINAL PAPER



Simulation of Hydromagnetic Williamson Nanofluid Flow with Melting Heat Transfer and Activation Energy Across a Porous Exponential Stretching Surface

K. Venkatadri 1 · G. Dharmaiah 2 · K. S. Balamurugan 3 · J. L. Rama Prasad 4 · Ali J. Chamkha 5

Accepted: 7 March 2025

© The Author(s), under exclusive licence to Springer Nature India Private Limited 2025

Abstract

Nanofluids have been shown to exhibit exceptional electrical and thermal conductivities, chemical and mechanical stability and physiochemical reliability in wide-ranging applications covering biomedicine, energy and aerospace. Motivated by emerging applications, the characteristics of a Williamson fluid flow containing nanoparticles are included in this study. The numerical examination of combined effects of Brownian motion, radiation, activation energy, suspended nanoparticles on hydromagnetic flow Williamson nanofluid over a melting sheet has been presented. To formulate the physical model mathematically, a set of connected partial differential frameworks is used. A bvp4c MATLAB solver is used to get the solutions of governed equations. In addition, calculated findings are compared with previously published publications, and high levels of consistency are noted. Besides, tabular data on shear stress, heat transfer coefficient, and concentration is shown. It can be shown that, when the Williamson parameter increases, the momentum boundary layer corpulence decreases, while the thermal and solutal boundary layers thickness increases. This study is closely related to metal spinning, drawing of plastic films, glass blowing, crystal growing, and cooling of filaments.

Keywords Williamson nanofluid · Exponential stretching surface · Chemical reaction · Magnetized fluid flow · Activation energy · Porous medium

Published online: 25 March 2025

⁵ Faculty of Engineering, Kuwait College of Science and Technology, 35004 Doha District, Kuwait



[☑] G. Dharmaiah dharma.g2007@gmail.com

Department of Mathematics, Mohan Babu University (Erstwhile Sree Vidyanikethan Engineering College), Tirupati, A.P. 517102, India

Department of Mathematics, Narasaraopeta Engineering College, Yellamanda, Narasaraopet, A.P. 522601, India

Department of Mathematics, RVR & JC College of Engineering, Guntur, A.P., India

⁴ Department of Mathematics, PB Siddartha College of Arts and Science, Vijayawada, A.P., India

74 Page 2 of 24 Int. J. Appl. Comput. Math (2025) 11:74

List of Symbols

 B_0 Radial magnetic field C_p Specific heat (J kg⁻¹ K⁻¹) C Nanoparticle volume fraction C_f Skin friction coefficient

 D_B Coefficient of Brownian diffusion

E Activation energy parameter

Dm Mass diffusion

 D_T Coefficient of thermophoretic diffusion

f Dimensionless stream function

Ha Hartmann number

g Gravitational acceleration

K Permeability

k Thermal conductivity of the fluid (W/mK)

*k** Mean absorption coefficient

Gr Grashof numberM Melting parameter

Nb Brownian motion parameterNt Thermophoresis parameterNu Heat transfer coefficient

Pr Prandtl number

R Radiation parameter T Fluid temperature (K) T_0 Reference temperature (K)

Le Lewis number S Suction parameter

Sh Sherwood number

 q_r Radiative heat flux (Jm⁻¹ s⁻¹) U Velocity of shrinking sheet λ Williamson fluid parameter

 K_r Reaction rate

U₀ Reference velocity

u, v Dimensionless velocity components in X and Y direction respectively (m/s)

V(x) Special type wall velocity

 V_0 Constant

X Stream wise coordinateY Transverse coordinate

Ec Eckert number Sc Schmidt number

Greek Symbols

 δ Temperature difference parameter

τ Ratio of nanofluid and base fluid heat capacity

 β Volumetric volume expansion coefficient of the fluid

 σ^* Stefan–Boltzmann constant



 $(\rho c)_p$ Nanoparticles heat capacity

 σ Electric conductivity of the fluid (S⁻¹)

 η Similarity variable (kg m⁻¹ s⁻¹)

 Γ Inertial drag coefficient

 $(\rho c)_f$ Base fluid heat capacity

 μ_f Dynamic viscosity (kg/ms)

 ξ Non-dimensional tangential coordinate

 ψ Non-dimensional stream function

 ν Kinematic viscosity (m² s⁻¹)

 ϕ Dimensionless concentration

 ρ Fluid density of the particles (kg/m³)

 θ Dimensionless temperature

Subscripts

- w Conditions on the wall
- ∞ Free stream condition
- α Thermal Diffusitivity
- σ_1 Chemical reaction parameter

Introduction

Non-Newtonian fluid analysis has attracted considerable attention in contemporary applied sciences like geothermal engineering, astrophysical bio-fluid analysis, geophysical analysis, and the petroleum industry. Applications based on the properties of non-Newtonian fluids can be found in the ceramics, wire coating, oils, printing, fiber engineering, and petroleum sectors. The rapid advancement of modern technology necessitates dramatic improvements in the area of temperature transmission. The flow and heat transfer properties of non-Newtonian fluids are important for numerous systems and a wide range of applications in the pharmaceutical, chemical engineering, and biotechnology industries, despite the inherent complexities of these fluids. Non-Newtonian fluids descripted by conservation theory in terms of their mechanical properties such as shear thinness and/or thickness, normal stress variations, and viscoelastic interactions; thus, sophisticated and effective foresight is required. Melting heat transfer involves the exchange of heat leading to a phase change from solid to liquid, governed by mechanisms such as conduction, convection, and sometimes radiation. The process is characterized by the absorption of latent heat at the melting point, where temperature remains constant while the phase change occurs. Key equations include Fourier's law for heat conduction and energy balance equations, while the Stefan problem models the moving boundary of the melting front. Applications span from cryogenics and thermal energy storage to climate studies and manufacturing processes, often requiring numerical methods like finite difference or finite element methods for accurate analysis and prediction.

The study of fluid dynamics is vitally important in a wide variety of manufacturing processes, as well as in the fields of chemical engineering, biomedicine, and advanced technology, particularly nanotechnology. Across order to gain a deeper comprehension of its rheology, a large number of researchers are focusing their efforts on developing explanations for the integrity of fluid dynamics. Researchers explored in engineering and science zeroed



emphasis on non-Newtonian fluids as a primary area of interest for their investigation. Non-Newtonian fluid qualities can be found in a wide variety of commercial liquids, including polycrystal melts, slurries, oils, paints, some fuels, paper products, paints, cosmetics, solutions, and slurries. The Williamson fluid is one of the most important non-Newtonian fluids. It is distinguished from other non-Newtonian fluids by the fact that its viscosity decreases as the rate of shear stress increases. Additionally, the Williamson fluid is extremely close to the properties of polymeric solutions, for instance. In a different sense, the Williamson fluid model predicts that the effective viscosity will decrease endlessly as the shear rate increases. This means that the viscosity will be infinite when the shear rate is steady, but it will become zero as the shear rate approaches infinity. However, the Williamson model was not taken into account in any of this research. This is a shear-thinning non-Newtonian model, and it models polymer viscoelastic flows pretty effectively throughout a broad spectrum of shear rates. When the shear stress rate increases, Williamson fluids have a decrease in their viscosity. The use of this paradigm in engineering simulations has gained considerable traction recently. Numerical analysis of the two-dimensional time-independent flow phenomenon of a Maxwell fluid carrying nanoparticles with the relevance of the magnetic dipole is performed by Kumar et al. [1] through a stretchy surface. The importance of physical boundary conditions in the bioconvection radiative flow problem of a non-Newtonian Maxwell fluid was investigated by Abdal et al. [2]. They saw that as the thermal radiation parameter increased, the Maxwell fluid's heat transfer rate did as well. The radiative flow mechanism produced by two stretchy disks in a Maxwell fluid was discussed by Chu et al. [3], who incorporated the two-phase Buongiorno model. Additional studies of oblique stagnation point flow that incorporate the effects of a wide variety of physical variables are covered in the cited works [4-8].

Real-world situations do not always require the surface, such as stretching plastic sheeting during installation. Over the past few years, heat transfer around continuous stretchable plane under surface temperature attracted a great deal of attention. This is due to the importance of the process in the industrial metal wires, paper production, and films. When making plastic, cooling in polymer is largely contingent on the characteristic of the eventual produce. This is also true in the manufacturing of polymer. From a manufacturing and industrial point of view, the quality of final items is significantly impacted by the presence of surfaces that have the property of stretching. Stretching sheet has a wide range of uses, including the spinning of metals, the fabrication of fibers, and extrusion. The transfer of heat via a stretching sheet is an important topic of research because of its application in a variety of technical and industrial projects, such as improving the capacity of paints for use in fibers and so on. This is due to its various and substantial uses in technological and industrial issues, including wire drawing, plastic sheet extrusion, hot rolling, metal spinning, and many others. Vaidya et al. [9] explored mass transfer and heat transfer implications on a hydromagnetic nanofluid were manifested as the fluid moved towards a nonlinearly stretched Riga plate. Vedavathi et al. [10] conducted a numerical investigation of Fluid flow in a non-darcy environment across a stretched regime under convective Nield's context with activation-energy. Dharmaiah et al. [11] conducted research on the topic of the influence of magnetohydrodynamic Radiation nonlinearities in micropolar nanofluids across a stretchable surface using Buongiorno's model. Multidimensional explores Williamson nanofluid through a medium containing Darcy-Forchheimer pores, a case of stretchable sheets of varying thicker ness, activation energy, binary chemical reactions were the subject of research carried out by Gautam et al. [12].

The activation energy of a material is defined as the lowest amount of energy it requires receive in order to undergo a particular chemical process and subsequent transformation. In order for a chemical reaction to take place, the reactants must supply an amount of energy



known as the activation energy. Oil storage, industrial engineering, geothermal production, base substances liquid mechanics, oil emulsification, and food production are just few of the many activation energy significances. New mass flux theory and the Arrhenius activation energy in a magnetically influenced Carreau nanofluid were theoretically analyzed by Irfan et al. [13]. Features of Activation Energy-Dependent, Multiple-Slip, and Hall Effect-Induced 3D Magneto-Convective Radiative Williamson Nanofluid Flow were reported by Nandi et al. [14]. Suganya et al. [15] provided a speciation of Cu-TiO₂ transport by activation energy significances. There is a critical role for melting and solidification phenomena in advanced technology processes. Melting phenomena of the solid–liquid phase shift have many applications, including welding, crystal formation, thermal protection, heat transfer, and permafrost melting [16–20].

The extinction of oscillatory velocity gradients caused by viscous strains is referred to as "viscous dissipation," which is a term that used in the field of fluid mechanics. It is the transformation of kinetic energy into the internal energy of the fluid. By converting the kinetic energy of an electric current into thermal energy, joule heating can also be called resistive heating or ohmic heating. The reason for this is that when an electric current travels through a solid or liquid conductor, the energy contained in the current is transformed into heat by resistances that form within the conductor. Here, free electrons exchange their energy through kinetic collisions. Ali et al. [21] investigated the dynamics of Soret–Dufour effects as well as the thermal features of Joule heating in numerous slips of Casson–Williamson nanofluid. Researchers Muhammad et al. [22] examined the thermal performance of Joule heating in Oldroyd-B nanomaterials while taking into consideration thermal-solutal convective circumstances. A study by Muhammad et al. [23] investigated Joule heating effect on nonlinear mixed convection radiative flows of Carreau nanofluid. Ali and Irfan [24] investigated the thermal characteristics of repeated slip and Joule heating in a Casson fluid with viscous dissipation and thermosolutal convective circumstances.

Many different fields have used fluid flow in porous media, including material refinement, heat energy, identified oil, and fuel mechanism. By combining heat transfer nanofluid boundary layer flows in permeable spaces with external magnetism, thermal performance can be improved. Many researchers have been focusing their attention on porous medium while attempting to solve a variety of difficulties. Porous media flow is especially important in following fields: material refinement, combustible cell mechanism, drying refinement, dribbling chromatography, and many more. By taking advantage of the magnetohydrodynamic boundary layer flow of a nanofluid across a porous medium, the combined effect of mass and heat transfer can be utilized to improve thermal performance.

This flow pattern is described as a magnetohydrodynamic boundary layer flow. The impact porous surfaces with heat and mass transfer, Navier slip appears on Walter's liquid B flow during thermal flow was described by Anusha et al. [25]. The viscous dissipation, radiant heating, and temperature-dependent viscosity of a CuAl₂O₃/H₂O hybrid nanofluid are all studied by Venkateswarlu and Narayana [26], as they follow the path of a stretched sheet through a porous media. Sharma [27] has modelled FHD flow and heat transfer due to the Coriolis force, viscous dissipation, and thermal radiation, over a rotating porous disc. Sharma et al. [28] proposed Flow of hydromagnetically heated boundary layers via a revolving disc through permeable media.

Williamson fluid and nanofluid have been studied independently in previous research along various geometries. This work consisted of taking various fluid properties documented a physical significance in various branches of the scientific community. Aim of the study is to elucidate a characteristics of nano Williamson flow fluid across non-linearly stretched regime that is inherent in permeable medium. This objective was arrived at after drawing motivation



from the studies that were successful and significant that were discussed earlier. The novelty of this paper is to examine Williamson nanofluid flow with melting heat transfer. The current flow problem has been set up mathematically in a manner that is consistent heat transfer and motion are fundamental laws. Governing equations transformed into nonlinear equations of the ordinary differential type by utilizing the similarity transformations. As a result, the nonlinear equations of the ordinary differential type with connected boundary conditions could be numerically solved by using the bvp4c package in MATLAB. Different flow factors are considered when examining the graphical behavior of the resulting equations. For a variety of physical flow parameters, the graphs have been constructed for distinct examined profiles. Fluid flow problems have risen in importance as a result of the widespread use of Williamson fluid flows over a stretching sheet in many different domains of science and industry. Making plastic and rubber sheets, creating glass fiber, melting spinning, and cooling metal plates are only a few more practical applications for this kind of research. Scientists have investigated its properties and behavior across a wide range of flow conditions, including how it reacts to heat transfer. Insights about Williamson fluid behavior gained from these studies can pave the way for new and useful technologies.

Here are a few research questions related to the simulation of hydromagnetic Williamson nanofluid flow with melting heat transfer and activation energy across a porous exponential stretching surface:

How does the magnetic field influence the velocity and thermal boundary layers in the flow of Williamson nanofluid over a porous exponentially stretching surface?

What is the effect of melting heat transfer on the thermal distribution and heat transfer rate in the presence of an exponentially stretching sheet?

How do activation energy and chemical reaction influence the concentration distribution and mass transfer characteristics of the nanofluid?

What role do Brownian motion and thermophoresis play in the heat and mass transfer behavior of the Williamson nanofluid?

How does the permeability of the porous medium affect the flow stability, skin friction, and heat transfer rate in the presence of a magnetic field?

Mathematical Foundation

Consider a steady two-dimensional flow of a non-Newtonian fluid, specifically the Williamson nanofluid, over an exponentially stretching surface that is embedded with a porous medium. Assume a viscous, incompressible fluid is moving across a flat sheet on the y = 0 plane. Assume that all of the flow is moving along y > 0. The wall is extended while the origin remains constant owing to the application of two equivalent and opposing forces along the x-axis. Physical structure interpretation is featured in Fig. 1. The induced magnetic field is ignored because of the small magnetic Reynolds number. This simplification lets us concentrate on the effects of a uniform magnetic field (B_0) applied perpendicular to the flow. Joule heating is a process in which heat dissipates in MHD flows of fluids. The Cauchy stress tensor, is entirely regulated via an additional stress tensor, is embodied in Williamson liquid (Refs. [8, 12, 14]).

The Cauchy stress tensor (\overline{S}) for the Williamson nanofluid is defined as [29]

$$\overline{S} = -p\overline{I} + \tau \tag{1}$$



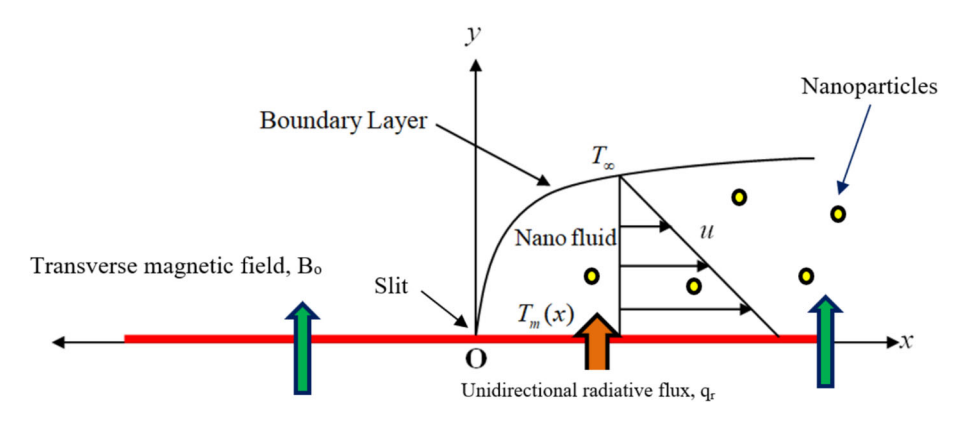


Fig. 1 Schematic of problem

$$\tau = \left[\mu_{\infty} + \frac{(\mu_0 - \mu_{\infty})}{1 - \Gamma \dot{\gamma}}\right] A_1 \tag{2}$$

where $(\mu_0, \mu_\infty) \to \text{limiting viscosity at zero and at an infinite shear rate, respectively, } \tau \to \text{extra stress tensor, } \overline{I} \to \text{unit tensor, } (\Gamma > 0) \to \text{time constant, } A_1 \to \text{first Rivlin-Erickson tensor, } p \to \text{pressure,}$

 $\dot{\gamma} \rightarrow is$ defined as

$$\dot{\gamma} = \sqrt{\frac{\pi}{2}}, \quad \pi = trace(A_1)^2 \tag{3}$$

here it is considered the case for $\Gamma V < 1$ and $\mu_{\infty} = 0$; thus, with help of Eq. (3), the Eq. (2) can expressed as follows:

$$\tau = \left[\frac{\mu_0}{1 - \Gamma \dot{\gamma}}\right] A_1 = \mu_0 (1 + \Gamma \dot{\gamma}) A_1 \tag{4}$$

The mathematical formulation is based on the following key assumptions:

Steady-State and Two-Dimensional Flow:

The flow is steady and two-dimensional over a stretching surface located at y = 0.

Williamson Non-Newtonian Fluid Model:

The fluid exhibits shear-thinning behavior.

The Williamson model is given by: $\tau = \left[\frac{\mu_0}{1-\Gamma\dot{\gamma}}\right]A_1 = \mu_0(1+\Gamma\dot{\gamma})A_1$.

Presence of Magnetic Field (MHD):

A uniform transverse magnetic field B_0 is applied in the y-direction.

The Lorentz force $-\sigma B_0^2 u$ opposes fluid motion.

Porous Medium:

The stretching sheet is embedded in a Darcy Brinckmann-type porous medium.

The drag force term is modeled as $-\frac{\mu}{k}u$, where K is the permeability of the porous medium. *Nanofluid Effects (Brownian Motion & Thermophoresis)*:

Nanoparticles exhibit Brownian motion and thermophoresis, affecting heat and mass transfer.

Melting Heat Transfer Condition:

The heat transfer at the surface is governed by a melting temperature T_m .



The solid surface melts into the fluid at a specific melting rate.

Activation Energy and Chemical Reaction:

The chemical reaction rate follows an Arrhenius-type expression:

$$-K_r \left(\frac{T}{T_{\infty}}\right)^n \exp\left(\frac{-E_a}{KT}\right) (C - C_{\infty})$$

The equations of motion for the associated quantities of momentum, energy, and continuity are (Ref. [8, 12, 14, 30])

$$\frac{\partial u}{\partial x} + \frac{\partial v}{\partial y} = 0 \tag{5}$$

$$u\frac{\partial u}{\partial x} + v\frac{\partial u}{\partial y} = \frac{1}{\rho}\frac{\partial}{\partial y}\left(\mu(T)\frac{\partial u}{\partial y} + \mu(T)\sqrt{2}\Gamma\left(\frac{\partial u}{\partial y}\right)^{2}\right) - \frac{\sigma B_{0}^{2}}{\rho}u - \frac{v}{k_{0}}u$$

$$\left(u\frac{\partial T}{\partial x} + v\frac{\partial T}{\partial y}\right) = \alpha_{m}\frac{\partial^{2}T}{\partial y^{2}} + \tau\left(D_{B}\frac{\partial T}{\partial y}\frac{\partial C}{\partial y} + \frac{D_{T}}{T_{\infty}}\left(\frac{\partial T}{\partial y}\right)^{2}\right)$$
(6)

$$+\frac{16\sigma^* T_{\infty}^3}{3k^*} \frac{\partial^2 T}{\partial y^2} + \frac{\mu}{\rho C_p} \left(\frac{\partial u}{\partial y}\right)^2 + \frac{\sigma B_0^2}{\rho C_p} u^2 \tag{7}$$

$$u\frac{\partial C}{\partial x} + v\frac{\partial C}{\partial y} = D_B \frac{\partial^2 C}{\partial y^2} + \frac{D_T}{T_\infty} \frac{\partial^2 T}{\partial y^2} - K_r \left(\frac{T}{T_\infty}\right)^n \exp\left(\frac{-E_a}{KT}\right) (C - C_\infty)$$
 (8)

here $\tau = \frac{(\rho c_p)_p}{(\rho c_p)_f}$, The corresponding boundary circumstances are (Ref [15, 21]):

$$u = U, \quad T = T_m, \quad k \left(\frac{\partial T}{\partial y}\right)_{y=0} = \rho(\lambda + c_s(T_m - T_0))v(x, 0), \quad C = C_m, \quad at \quad y = 0$$

$$u \to 0, \quad T \to T_\infty, \quad C \to C_\infty, \quad at \quad y = \infty$$

$$(9)$$

here $V(x) = V_0 e^{\frac{x}{2L}}$ specified as the suction velocity if V(x) > 0 and the blowing velocity if V(x) < 0, also $U = -U_0 e^{\frac{x}{L}}$ indicate the shrinking/stretching velocity, U_0 is the reference velocity. The mathematical model of temperature dependent viscosity model used by [31].

The similarity transformations are:

$$\eta = y\sqrt{\frac{U_0}{2\nu L}}\exp\left(\frac{x}{2L}\right), \quad \psi = \sqrt{2\nu L U_0}f(\eta)\exp\left(\frac{x}{2L}\right), \quad \alpha_m = \frac{k_m}{(\rho c)_f},$$

$$u = U_0\exp\left(\frac{x}{L}\right)f'(\eta), \quad v = \sqrt{\frac{\nu U_0}{2L}}\exp\left(\frac{x}{2L}\right)\left(f(\eta) + \eta f'(\eta)\right),$$

$$T - T_\infty = T_0\theta(\eta)\exp\left(\frac{x}{2L}\right), \quad C - C_\infty = C_0\phi(\eta)\exp\left(\frac{x}{2L}\right),$$

$$Ec = \frac{U_w^2}{C_p(T_\infty - T_m)}; \quad K_p = \frac{v}{k_0a}; \quad v = \frac{E_a}{k_f T_\infty}; \quad \sigma_1 = \frac{K_r^2}{a}$$
(10)

In this study, the equation for the dimensionless viscosity μ is generalized for the temperature dependence as follows [31]:

$$\mu(T) = \mu_{\infty} e^{-\alpha \theta} \tag{11}$$

Also, the stream function ψ is expressed as:

$$u = \frac{\partial \psi}{\partial y}, \ v = -\frac{\partial \psi}{\partial x} \tag{12}$$



By using the above-mentioned similarity changes, obtained the following similar equations:

$$e^{-\alpha \theta} \left[\left(1 + \lambda f'' \right) f''' - \alpha \theta' f'' \left(1 + 0.5 \lambda f'' \right) \right] + f f'' - 2 f'^2 - Ha \ f' - Kp \ f' = 0 \ \ (13)$$

$$\frac{1}{\Pr}\left(1 + \frac{4R}{3}\right)\theta'' + f\theta' - f'\theta + Nb\theta'\phi' + Nt\theta'^2 - Ecf'' + EcHaf'^2 = 0$$
 (14)

$$\phi'' + Sc(f\phi' - f'\phi) + \frac{Nt}{Nb}\theta'' - Sc\sigma_1(1 + \delta\theta)^n \exp\left(\frac{-E}{1 + \delta\theta}\right)\phi = 0$$
 (15)

The boundary constraints for above noticed similar equations are:

$$\Pr f(0) + M\theta'(0) = 0, \quad f'(0) = 1, \quad \theta(0) = 1, \quad \phi(0) = 1$$

$$f'(\infty) = 0, \quad \theta(\infty) = 0, \quad \phi(\infty) = 0$$
(16)

The non-dimensional quantities are as follows:

$$\begin{split} Ha &= \frac{2L\sigma B_0^2}{\rho U_0 c_p}, \quad Sc = \frac{\nu}{D_B}, \quad Nb = \frac{D_B \tau C_0}{\nu}, \quad \lambda = \Gamma \sqrt{\frac{U_0^3 \exp\left(\frac{3x}{L}\right)}{\nu L}}, \quad Nt = \frac{D_T \tau T_0}{T_\infty \alpha \nu}, \\ M &= \frac{c_p (T_m - T_\infty)}{\lambda + c_s (T_m - T_0)}, \quad K = \frac{2\nu L \exp\left(\frac{x}{2L}\right)}{\rho k_0}, \quad R = \frac{4\sigma T_\infty^3}{k k^*} \end{split}$$

The shear stress and wall heat stress on the permeable sheet are defined as follows:

$$Cf = \frac{2\tau_w}{\rho U_w^2}, \quad Nu = \frac{Lq_w}{(T_w - T_\infty)k}, \quad Sh = \frac{Lq_m}{(C_w - C_\infty)D}$$
 (17)

The terms τ_w , q_w and q_m are meant as below

$$\tau_w = \mu(T) \left(\frac{\partial u}{\partial y}\right)_{y=0} + \frac{\Gamma}{\sqrt{2}} \left(\frac{\partial u}{\partial y}\right)_{y=0}^2, \ q_w = k \left(\frac{\partial T}{\partial y}\right)_{y=0}, \ q_m = D \left(\frac{\partial C}{\partial y}\right)_{y=0}$$
(18)

Dimensionless forms of Cf, Nu and Sh are

$$\sqrt{\text{Re}_{x}}Cf = -2\left(f''(0) + \frac{\lambda}{2}(f''(0))^{2}\right)e^{-\alpha\theta}, \quad \frac{Nu}{\sqrt{\text{Re}_{x}}} = -\left(1 + \frac{4}{3}Rd\right)\theta'(0), \quad \frac{Sh}{\sqrt{\text{Re}_{x}}} = -\phi'(0)$$

$$\text{Re}_{x} = \sqrt{\frac{2U_{0}L}{\upsilon_{\infty}}}e^{x/L}$$
(19)

Method of Solution

To solve the difficult 2-point boundary value issue given by Eqs. (7) and (8), by the help of BVP4C scheme in combination with the shooting performance of integration. Here, the nonlinear ODEs are solved numerically by BVP4C scheme. The CPU time to compute profile values is $1.78 \, \text{s}$, and the error tolerance is 10^{-6} . The schema chart is modeled in Fig. 2.



74 Page 10 of 24 Int. J. Appl. Comput. Math (2025) 11:74

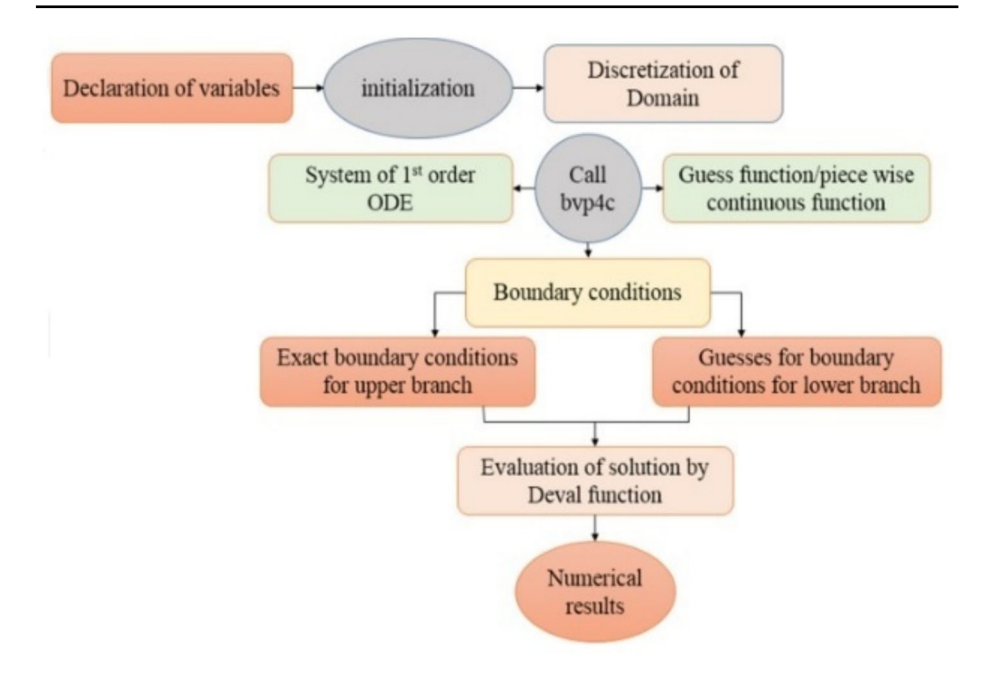


Fig. 2 Numerical solution algorithm flow chart

Table 1 Assessment values for $-\theta'(0)$ for Pr

Pr	Mukhopadhyay and Gorla [32]	Present study	
1.0	0.9547	0.9550	
2.0	1.4714	1.4715	
3.0	1.8691	1.8692	
5.0	2.5001	2.4999	
10.0	3.6603	3.6602	

Numerical Validations

For the purpose of validating the correctness of our method, the findings of this examination are compared to those available from text, and a remarkable quantity of consistency is seen. An essential to emphasize the fact that the existing model equations reduced to work by Mukhopadhyay and Gorla [32] for $-\theta'(0)$, for various values of Pr with Ec = Nt = Nb = 0. Comparisons are exposed in Table 1. This table demonstrates that the current findings are in magnificent accord about previous work that has been published.

Results and Discussion

The current research uses the default settings for the following parameters in all computations: Here the fixed values are: $\alpha = 0.5$; $\lambda = 0.2$; Ha = 1.0; K = 0.2; Pr = 0.71; Ec = 0.5; Nt = 0.5; Nb = 0.5; R = 0.2; Sc = 1.4; $\sigma_1 = 0.1$; $\delta = 1$; E = 1; n = 0.1; Me = 0.1.



Figure 3 displays the influence of thermal diffusivity (α) on velocity distribution. t is revealed that velocity diminishes with an escalation in thermal diffusivity (α). Rate of change in temperature as a result of heating or cooling is quantified by a property called thermal diffusivity. Substances with a low thermal diffusivity take longer to heat up or cool down than those with a higher value. The impact of Ha on $f'(\eta)$ fields is illustrated in Fig. 4. It is revealed that velocity diminishes with an escalation in Ha. This notifies that increase in magnetic field obtains the resistive force (Lorentz force) leading to a reduction in the fluid velocity. This also means a reduction in the thickness of the thermal boundary layer. The heat generated causes resistance of the fluid for a greater value of Ha, which escalates the fluid temperature, and similar behaviour is also seen for the concentration field. In magnetohydrodynamic research, these phenomena are extensively documented by [24, 25]. Figure 5 presents the disparity of permeable parameter K on $f'(\eta)$ field. Figure 5 displays the enhancing values of permeable parameter K on velocity field. Here, velocity declines with a larger value of K. This is because enhancing values of K lessens that This medium introduces resistance and impediments to the fluid's movement. Figure 6 presents Williamson fluid parameter (λ) on $f'(\eta)$ sketch. The $f'(\eta)$, is seen to lessen with improving Williamson fluid parameter (λ) values. Physically, by lowering the momentum boundary layer denseness. Furthermore, radiation continuance and viscous dissipation processes, along with the nonlinearly expanding sheet, yields the fluid's motion. Figure 7 demonstrates the impact of thermal radiation parameter on the temperature profile. observed enhancement in temperature field with higher value of radiation parameter. Physically R is the relative involvement of heat transmission conduction to thermal radiation transfer. Augmentation in R generates more heat which turn increases the nanofluid temperature. The impacts parameter Nb and parameter Nt on the $\theta(\eta)$ are elucidated in Figs. 8 and 9. Enhancing Nb leads to the faster random motion of nanoparticles in fluid flow which

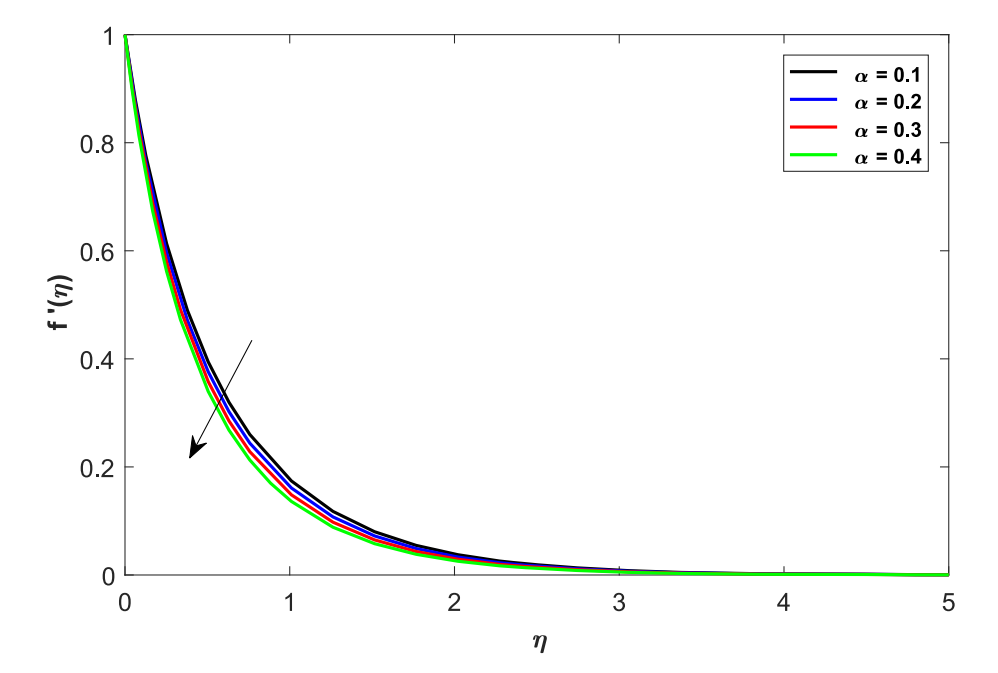


Fig. 3 Performance of α on velocity



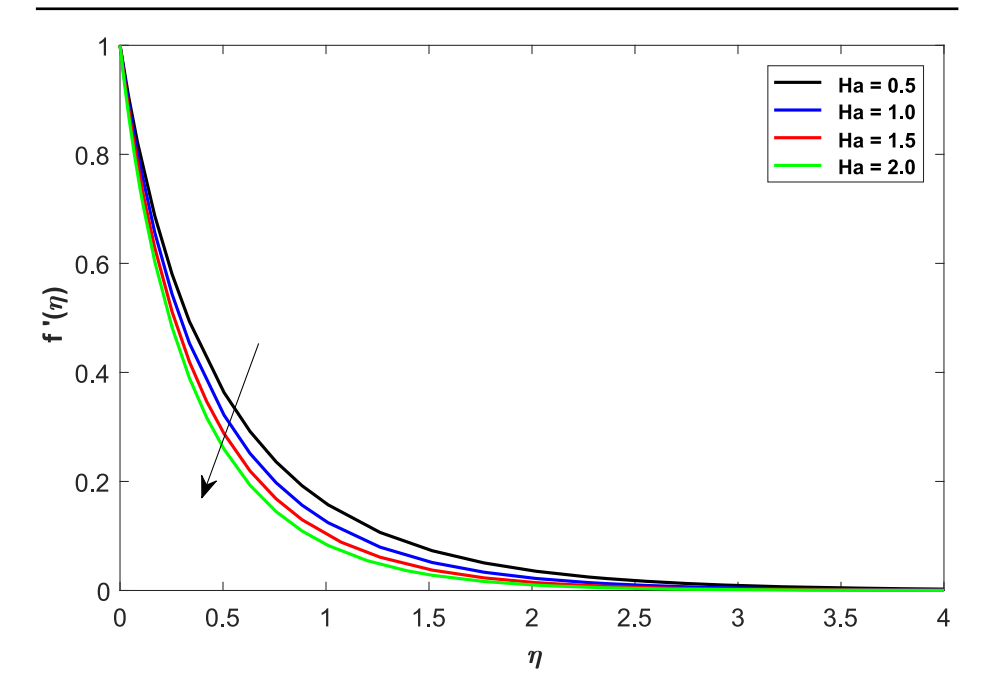


Fig. 4 Performance of Ha on velocity

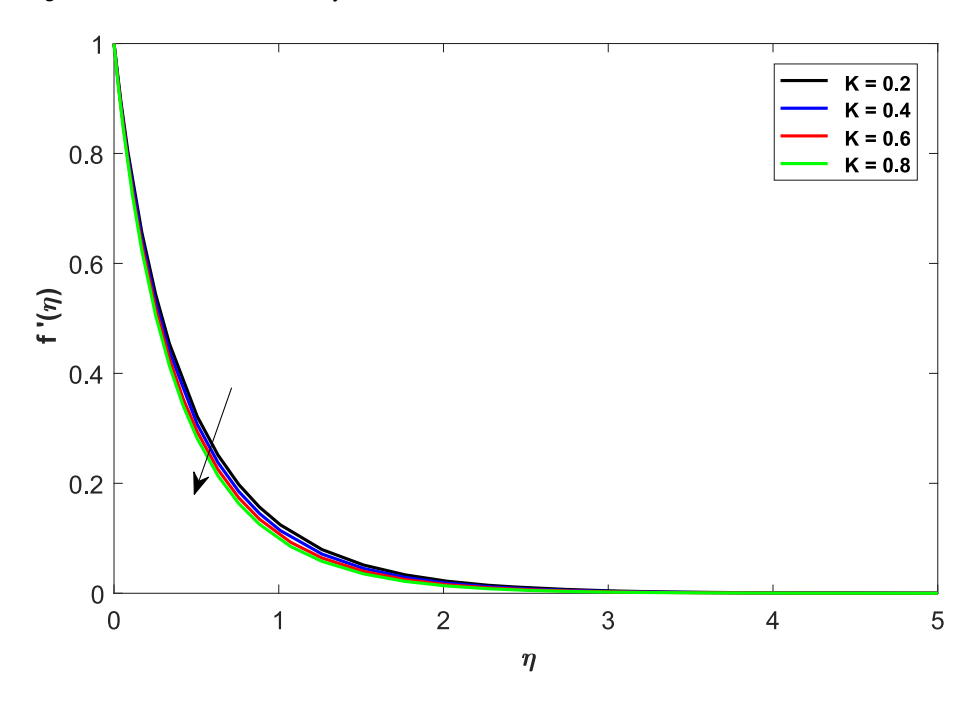


Fig. 5 Performance of K on velocity



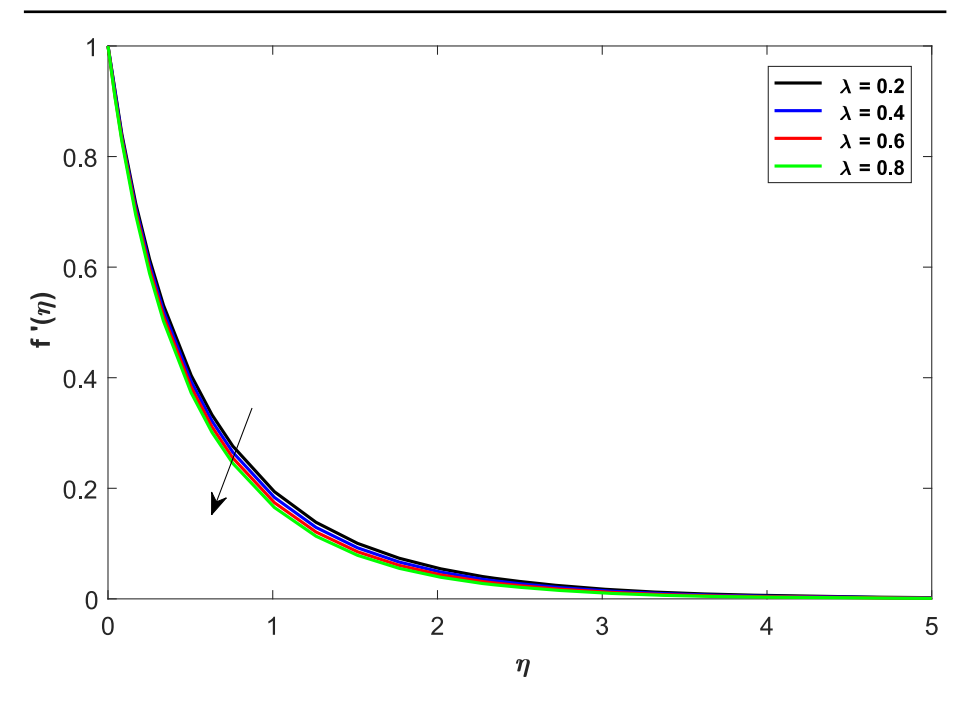


Fig. 6 Performance of λ on velocity

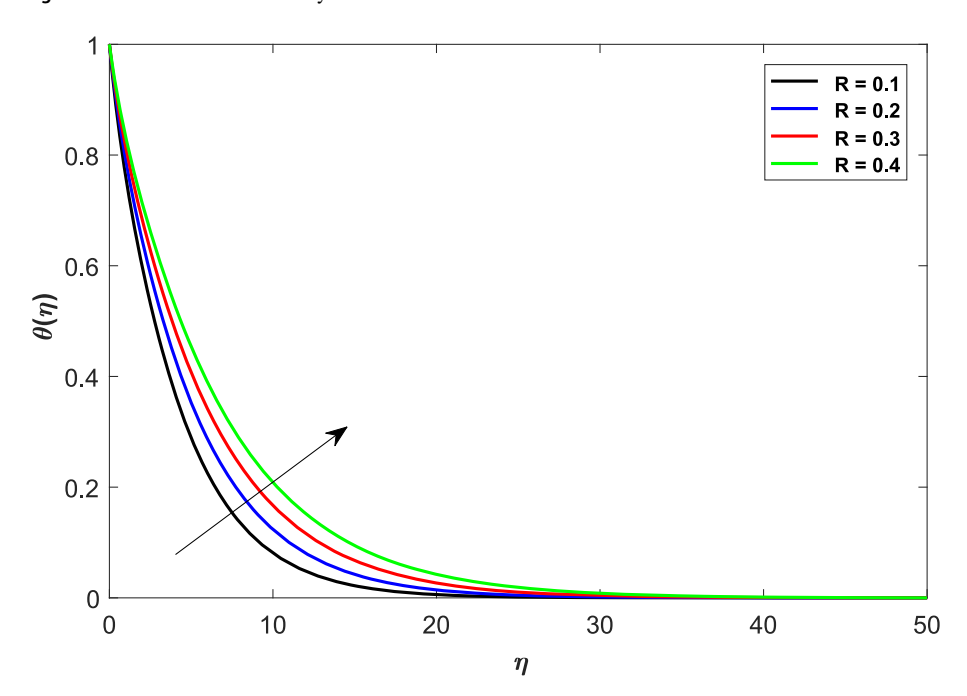


Fig. 7 Performance of R on $\theta(\eta)$

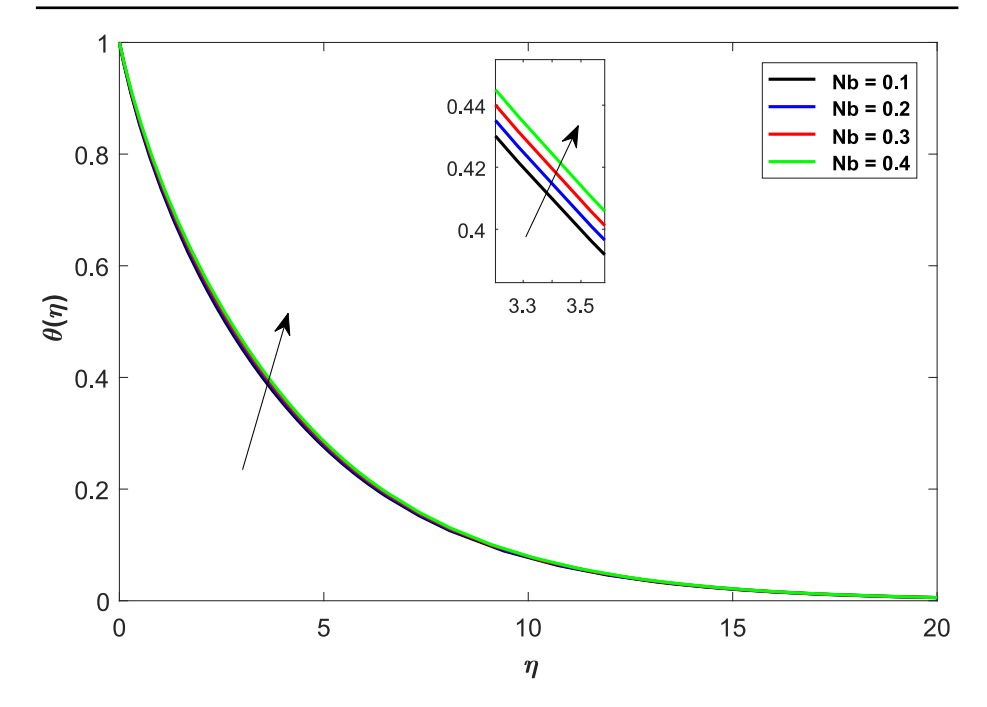


Fig. 8 Performance of Nb on temperature

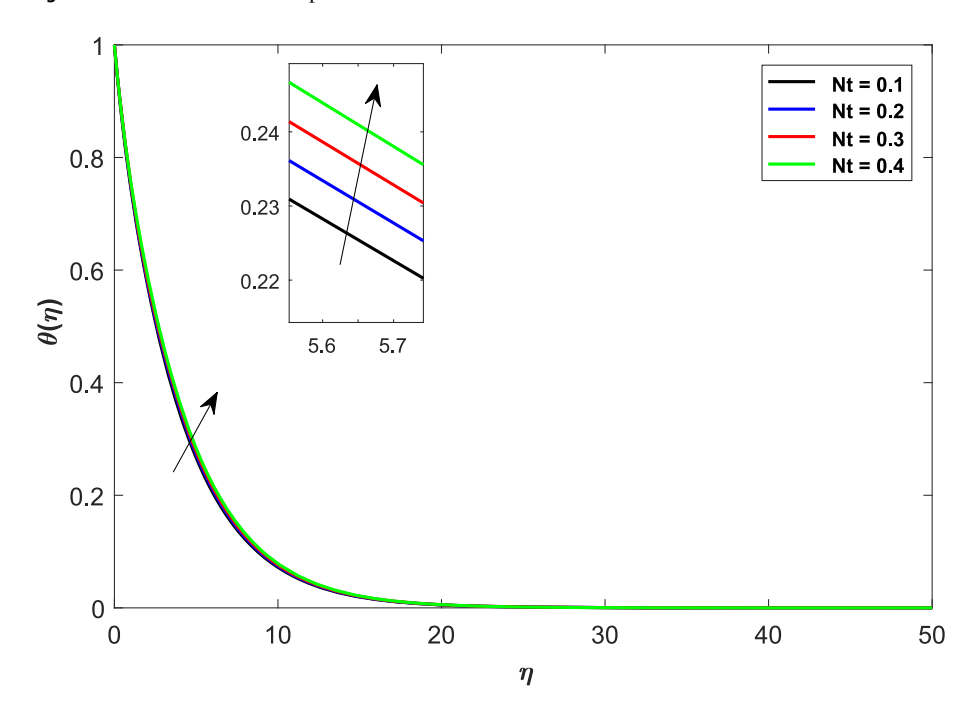


Fig. 9 Performance of Nt on $\theta(\eta)$



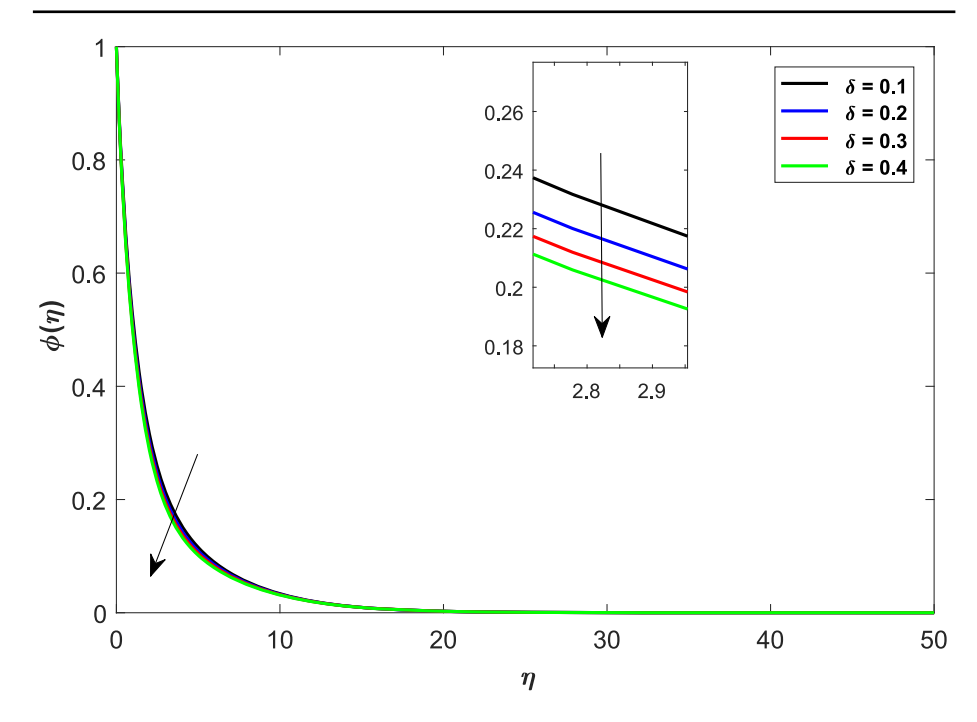


Fig. 10 Performance of δ on $\varphi(\eta)$

displays an extension in thermal boundary layer thickness and augments the temperature of nanofluid more rapidly. A similar configuration is perceived for growing values Nt on θ (η). As in procedure of thermophoresis, more heated particles near the surface travel away from heated regions toward the cold region and rise temperature there and collective temperature of the whole system rises. Effect of δ on θ (η) is presented in Fig. 10. Clearly temperature is a decreasing function of δ . The impact of activation energy parameter E on concentration $\varphi(\eta)$ is presented in Fig. 11. The higher value of activation energy augmented the concentration $\varphi(\eta)$ of nanofluid. Figure 12 is sketch to examine the behavior of reaction rate $\sigma 1$ on $\varphi(\eta)$. It is observed that concentration $\varphi(\eta)$ is decreasing function for σ_1 . The influences of parameter (Nb) and parameter (Nt) on the concentration profle $\varphi(\eta)$ are elucidated in Figs. 13 and 14. Increasing value of (Nb) reduces $\varphi(\eta)$ while increasing (Nt) augmented $\varphi(\eta)$. Boosting (Nt) enhances the motion of nanoparticles from higher to lower temperature gradient which in turn, exploit the concentration of nanoparticles. Figure 15 is drawn to scrutinize the behavior of Sc on $\varphi(\eta)$. Increasing Sc the mass diffusivity decays and thus concentration is declined. Figures 16, 17 and 18 describes the profiles for velocity, temperature and concentration for various melting parameter (M) values. An increase in M is observed to decrease the velocity profiles slightly. It is also found that the thermal and concentration boundary layer thickness are also reduced with greater M values. Growth of melting therefore inhibits all diffusion types in the boundary layer i.e. momentum, thermal and nanoparticles species and neglect ion of this effect in materials processing simulations leads to an over-estimate in velocity, temperature and nanoparticles volume fraction characteristics.

The variation of the skin friction, Nusselt number, Sherwood numbers are shown Tables 2, 3 and 4 for various values of the governing parameters. The increased shear stress is generally a disadvantage in applications. The negative value of skin friction means that the plate exerts a



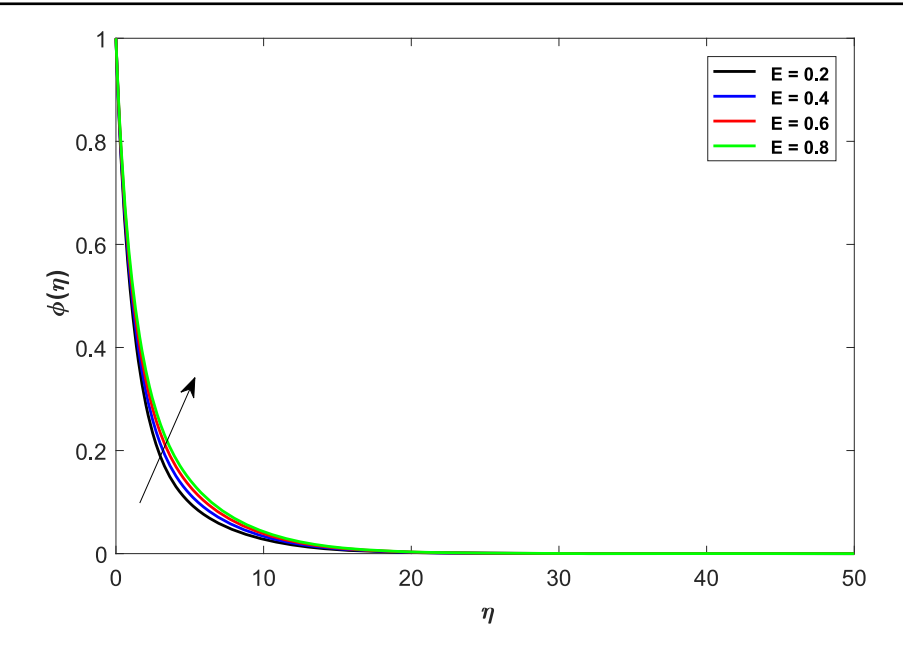


Fig. 11 Performance of E on $\phi(\eta)$

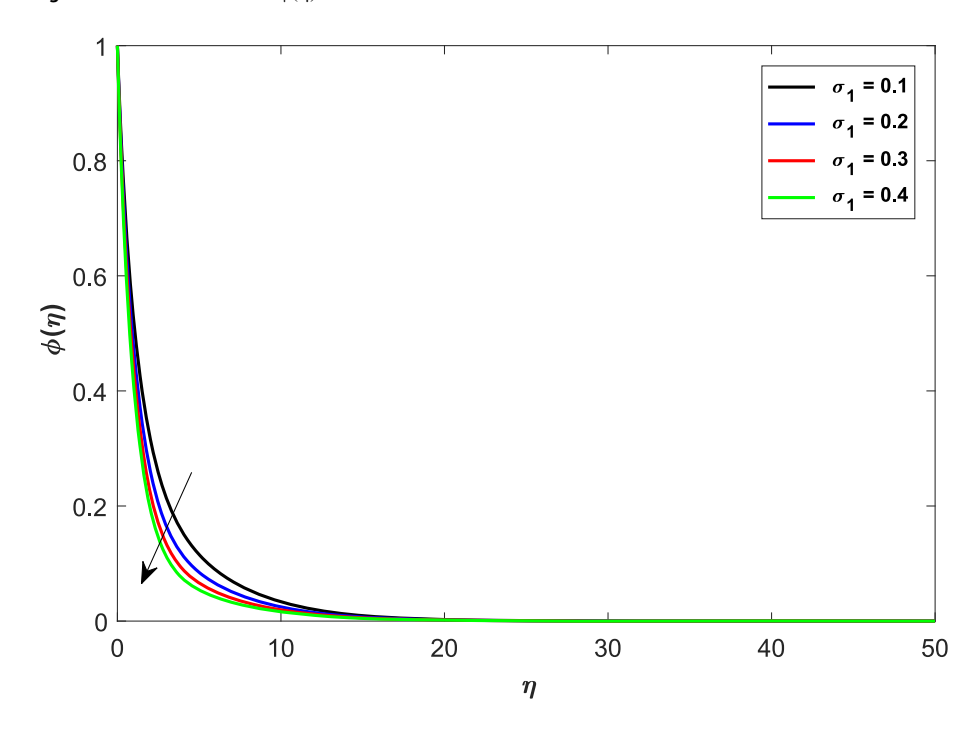


Fig. 12 Appearance of σ_1 on concentration



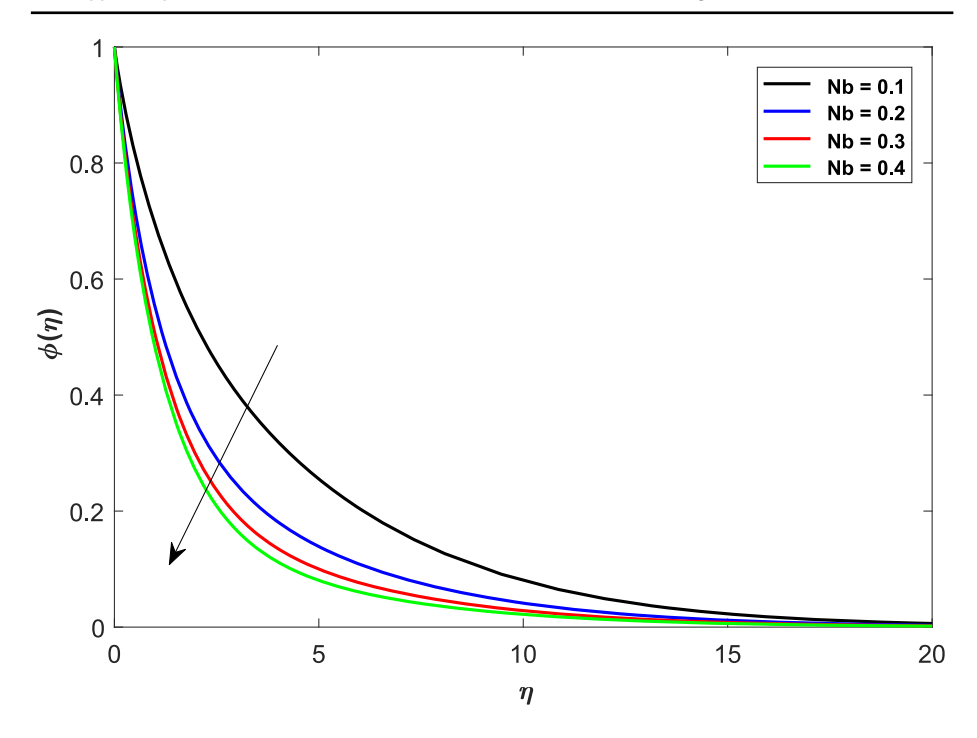


Fig. 13 Appearance of Nb on concentration

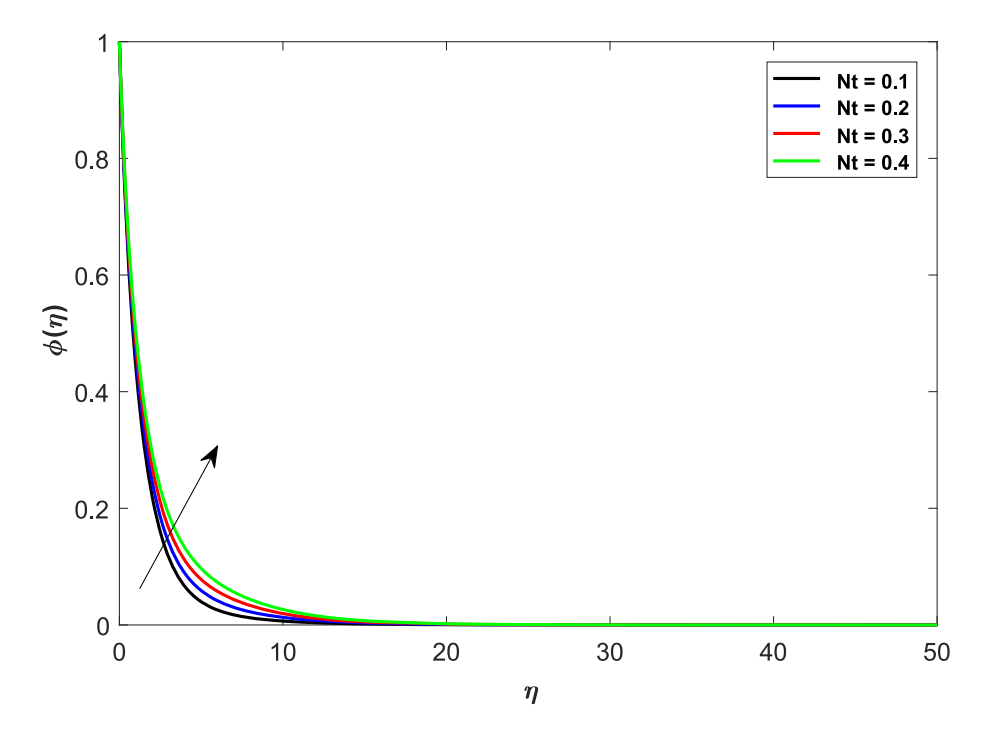


Fig. 14 Performance of Nt on $\phi(\eta)$

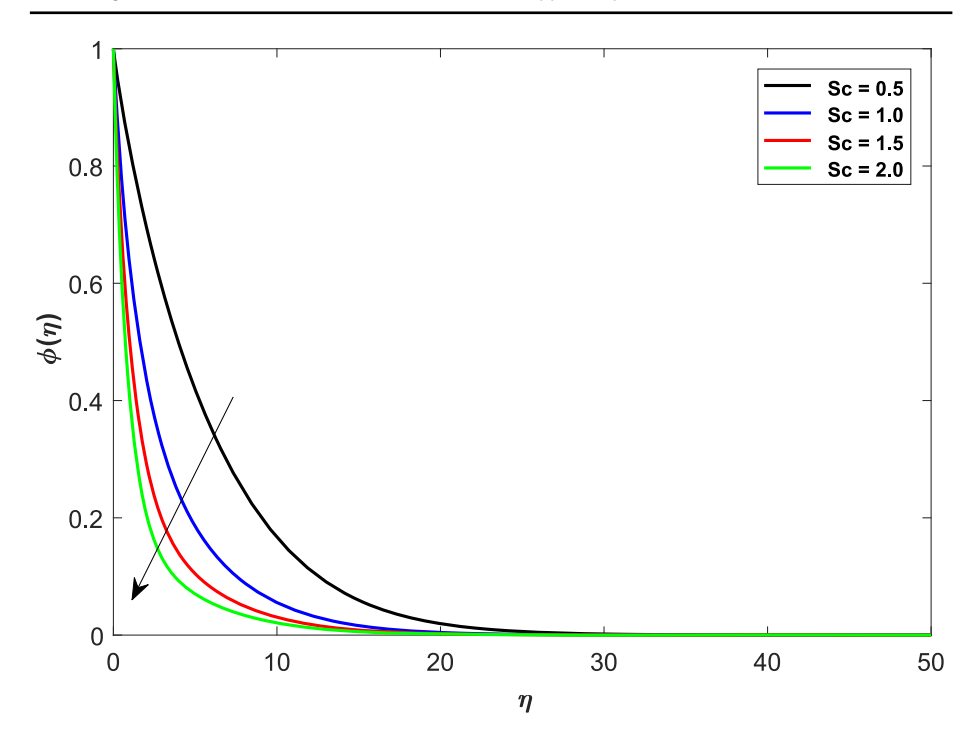


Fig. 15 Performance of Sc on $\varphi(\eta)$

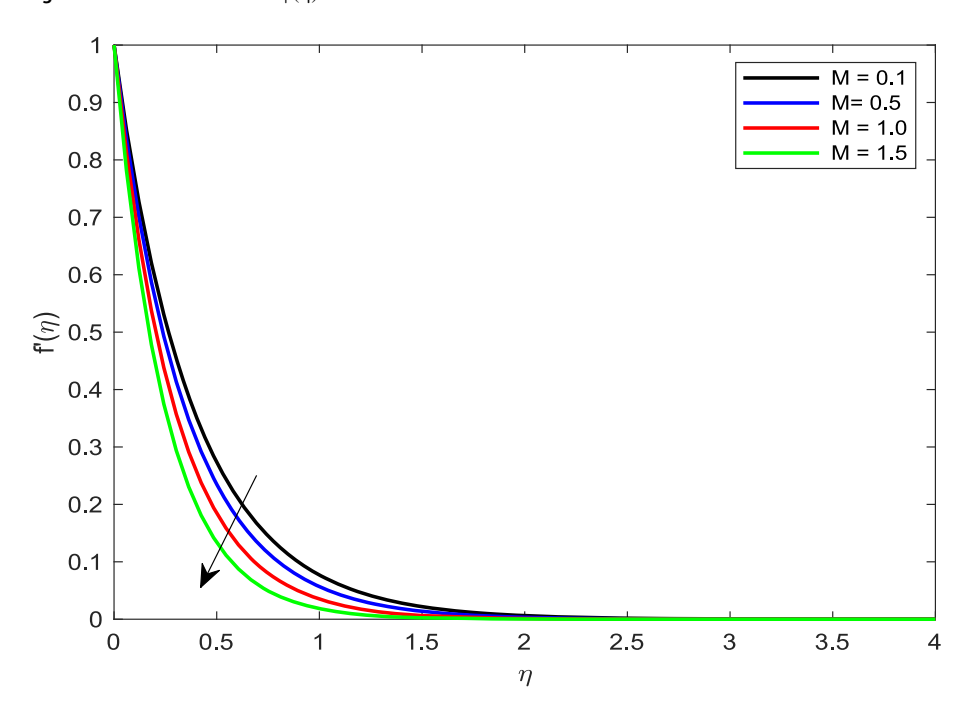


Fig. 16 Performance of M on velocity



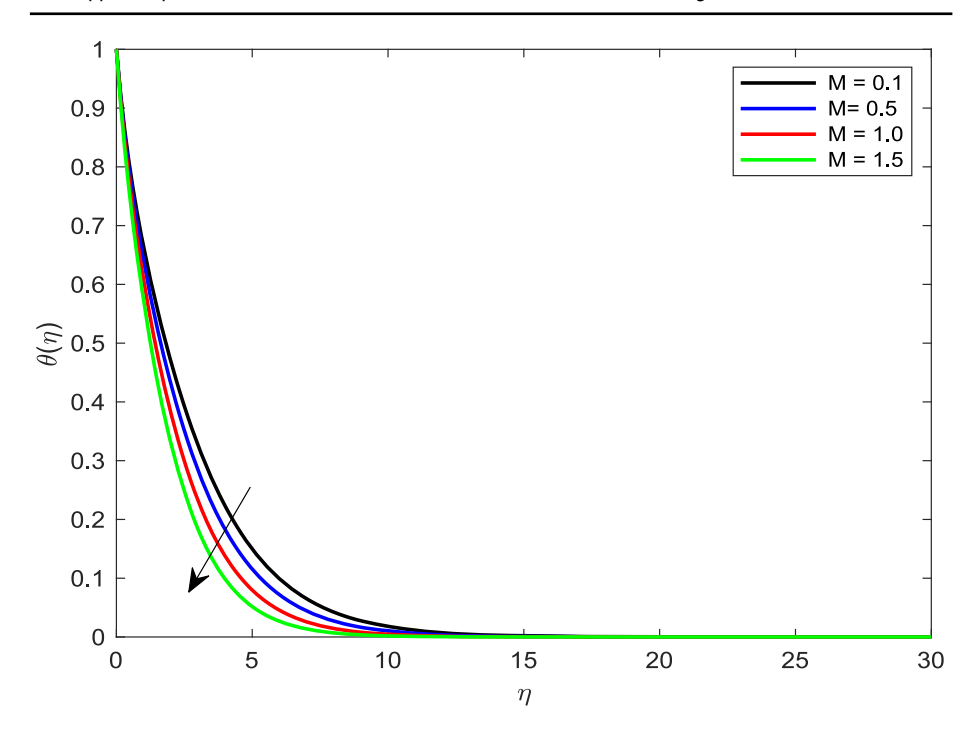


Fig. 17 Performance of M on $\theta(\eta)$

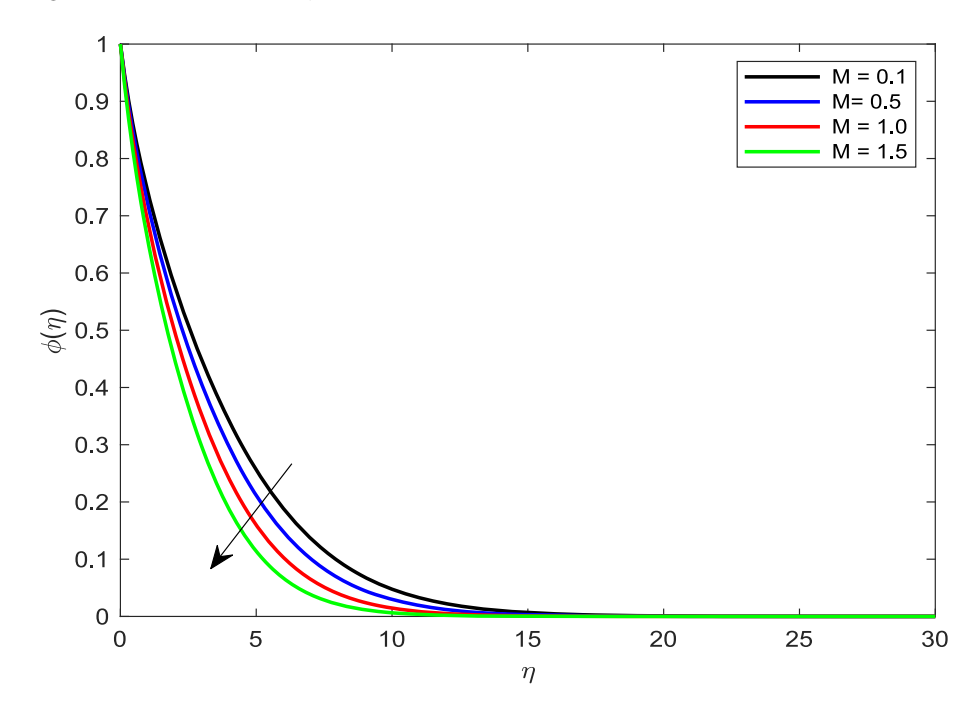


Fig. 18 Performance of M on $\varphi(\eta)$



Table 2 Cf values for distinct values with $\alpha = 0.5$; $\lambda = 0.2$; Ha = 1.0; K = 0.2; Pr = 0.71; Ec = 0.5; Pr = 0.71; Ec = 0.5; Pr = 0.71; Ec = 0.7; Ec =

α	λ	На	K	Me	Cf
0.1 0.2 0.3 0.4					2.096318 2.241459 2.398925 2.571041
	0.2 0.4 0.6 0.8				2.400313 2.760852 2.832459 2.915874
		0.5 1.0 1.5 2.0			2.429038 2.760852 3.100488 3.464853
			0.2 0.4 0.6 0.8		2.760852 2.894972 3.031180 3.170726
				0.1 0.2 0.3 0.4	2.760852 2.760853 2.760854 2.760855

Table 3 Nu values for distinct values with $\alpha = 0.5$; $\lambda = 0.2$; Ha = 1.0; K = 0.2; Pr = 0.71; Ec = 0.5; Nt = 0.5; Nb = 0.5; R = 0.2; Sc = 1.4; $\sigma_1 = 0.1$; $\delta = 1$; E = 1; n = 0.1; Me = 0.1

R	Nt	Nb	Ec	Nu
0.1 0.2 0.3 0.4				0.374331 0.388377 0.400528 0.411147
	0.1 0.2 0.3 0.4			0.409675 0.404122 0.398725 0.393478
		0.1 0.2 0.3 0.4		0.437412 0.424542 0.412085 0.400034
			0.1 0.3 0.5 0.7	0.388377 0.236088 0.083221 - 0.070237



Table 4 *Sh* values for distinct values with $\alpha = 0.5$; $\lambda = 0.2$; Ha = 1.0; K = 0.2; Pr = 0.71; Ec = 0.5; Ec =

Sc	Nt	Nb	σ_1	δ	E	Sh
0.22 (hydrogen)						- 0.021093
0.62 (water vapour)						0.333551
0.78 (ammonia)						0.449506
	0.1					0.960262
	0.2					0.925497
	0.3					0.891806
	0.4					0.859136
		0.1				0.004119
		0.2				0.519743
		0.3				0.691143
		0.4				0.776494
			0.1			0.827437
			0.3			0.983765
			0.5			1.101436
			0.7			1.200768
				0.2		0.800872
				0.4		0.808819
				0.6		0.815792
				0.8		0.821953
					0.1	0.888989
					0.3	0.873734
					0.5	0.859389
					0.7	0.845942

drag force on the fluid. From Table 2 concludes that the skin-friction enhances with increase in α , λ , Ha, K and Me. From Table 3 concluded that the Nusselt number enhance with increase in R while decrease when increasing of Nt, Nb and Ec. Sherwood number is decreasing tendency with Sc and E while raises of Nt, Nb and σ_1 .

Conclusions

The numerical examination of combined effects of Brownian motion, radiation, activation energy, suspended nanoparticles on hydromagnetic flow Williamson nanofluid over a melting sheet has been presented. To formulate the physical model mathematically, a set of connected partial differential frameworks is used. A bvp4c MATLAB solver is used to get the solutions of governed equations. Furthermore, an affirmation of solutions with previously studies, included. The observations are shown as:

- 1. For greater value of Ha the Lorentz forces enhances which rises the resistive force to the nanofluid motion and in result the velocity reduces.
- The motion of a Williamson fluid with variable viscosity is more affected by the magnetic
 field than the motion of a Williamson fluid with constant characteristics. Additionally, compared to Williamson fluid with constant values, the viscous zone is shorter
 in Williamson fluid than viscosity and thermal conductivity.



74 Page 22 of 24 Int. J. Appl. Comput. Math (2025) 11:74

Higher values of melting parameter consistently decelerate the boundary layer flow and suppress temperature and nanoparticle concentration.

- 4. Thermal conductance increases when temperature causes an increase in thermal conductance. However, it is noted that the thermal conductance of a fluid of constant viscosity is greater than the thermal conductance of a fluid of variable viscosity.
- Enhancing Nb leads to the faster random motion of nanoparticles in fluid flow which displays an extension in thermal boundary layer thickness and augments the temperature of nanofluid more rapidly.
- A decrement in concentration values is observed with greater Schmidt number (lower molecular diffusivity of the diffusing species) and chemical reaction rate parameter.
- 7. Nusselt number (heat transfer rate at the stretching wall) is reduced with higher magnetic.
- The Joule heating results in an increase in the temperature of the fluids with constant and variable diffusion coefficients

Future Scope

The main focus of this work is theoretical, and it will be built upon a thorough examination of the pertinent mathematical models. Believe that this work will have significant ramifications for a variety of commercial applications and contribute to the illumination of the intriguing interactions between polymers and nanoparticles in fluids. In the end, Hope this study will act as a foundation for more research in this fascinating field.

Acknowledgements The authors are grateful to the reviewers for their comments which have improved the clarity of the present study.

Author Contributions Conceptualization—J. L. Rama Prasad; Methodology—K. S. Balamurugan; Supervision—K. S. Balamurugan and Ali J. Chamkha; Validation—G. Dharmaiah; Writing-original draft—G. Dharmaiah; Dr. K. Venkatadri Writing-review and editing—Dr. K. Venkatadri, K. S. Balamurugan and Ali J. Chamkha; All authors have read and agreed to the published version of the manuscript.

Funding This research received no specific grant from any funding agency in the public, commercial, or not-for-profit sectors.

Data Availability No data were generated or analyzed for this current study.

Declarations

Conflict of interest The authors declare that they have no conflict of interest.

References

- Kumar, V., et al.: Analysis of single and multi-wall carbon nanotubes (SWCNT/MWCNT) in the flow of Maxwell nanofluid with the impact of magnetic dipole. Comput. Theor. Chem. 1200, 113223 (2021)
- Abdal, S., et al.: On development of heat transportation through bioconvection of Maxwell nanofluid flow due to an extendable sheet with radiative heat flux and prescribed surface temperature and prescribed heat flux conditions. Math. Methods Appl. Sci. (2021). https://doi.org/10.1002/mma.7722
- Chu, Y.M., et al.: Thermophoretic particles deposition features in thermally developed flow of Maxwell fluid between two infinite stretched disks. J. Mater. Res. Technol. 9(6), 12889–12898 (2020)
- Irfan, M.: Energy transport phenomenon via Joule heating and aspects of Arrhenius activation energy in Maxwell nanofluid. Waves Random Complex Media (2023). https://doi.org/10.1080/17455030.2023.21 96348



- Irfan, M.: Influence of thermophoretic diffusion of nanoparticles with Joule heating in flow of Maxwell nanofluid. Numer. Methods Partial Differ. Equ. 39, 1030–1041 (2023). https://doi.org/10.1002/num.22920
- Rafq, K., Irfan, M., Khan, M., Anwar, M.S., Khan, W.A.: Arrhenius activation energy theory in radiative flow of Maxwell nanofluid. Phys. Scr. 96(4), 045002 (2021). https://doi.org/10.1088/1402-4896/abd903
- Irfan, M., Khan, M., Khan, W.A.: Heat sink/source and chemical reaction in stagnation point flow of Maxwell nanofluid. Appl. Phys. A 126, 892 (2020). https://doi.org/10.1007/s00339-020-04051-x
- Gangadhar, K., Seshakumari, P.M., Rao, M.V.S., Chamkha, A.J.: MHD Flow analysis of a williamson nanofluid due to Thomson and Troian slip condition. Int. J. Appl. Comput. Math. (2022). https://doi.org/ 10.1007/s40819-021-01204-1
- Vaidya, H., et al.: Mixed convective nanofuid fow over a non linearly stretched Riga plate. Case Stud. Termal Eng. 24, 100828 (2020)
- Vedavathi, N., Dharmaiah, G., Venkatadri, K., Abdul Gaffar, S.K.: Numerical study of radiative nondarcy nano fluid flow over a stretching sheet with a convective nield's conditions and energy activation. Nonlinear Eng. 10, 159–176 (2021)
- Dharmaiah, G., Makinde, O.D., Balamurugan, K.S.: Influence of magneto hydro dynamics (MHD) nonlinear radiation on micropolar nanofluid flow over a stretching surface: revised buongiorno's nanofluid model. J. Nanofluids 11(6), 1009–1022 (2022)
- Gautam, A.K., Verma, A.K., Bhattacharyya, K., Mukhopadhyay, S., Chamkha, A.J.: Impacts of activation energy and binary chemical reaction on MHD Flow of Williamson nanofluid in Darcy–Forchheimer porous medium: a case of expanding sheet of variable thickness. Waves Random Complex Media (2021). https:// doi.org/10.1080/17455030.2021.1979274
- Irfan, M., Rafiq, K., Khan, M., Waqas, M., Anwar, M.S.: Theoretical analysis of new mass flux theory and Arrhenius activation energy in Carreau nanofluid with magnetic influence. Int. Commun. Heat Mass Transf. 120, 105051 (2021). https://doi.org/10.1016/j.icheatmasstransfer.2020.105051
- Nandi, S., Kumbhakar, B., Seth, G.S., Chamkha, A.J.: Features of 3D magneto-convective nonlinear radiative Williamson nanofluid flow with activation energy, multiple slips and hall effect. Phys. Scr. 96, 065206 (2021). https://doi.org/10.1088/1402-4896/abf009
- Suganya, S., Muthtamilselvan, M., Alhussain, Z.A.: Activation energy and Coriolis force on Cu— TiO2/water hybrid nanofluid flow in an existence of nonlinear radiation. Appl. Nanosci. 11, 933–949 (2021)
- Singh, K., Pandey, A.K., Kumar, M.: Melting heat transfer assessment on magnetic nanofluid flow past a porous stretching cylinder. J. Egypt. Math. Soc. 29, 1 (2021). https://doi.org/10.1186/s42787-020-00 109-0
- Song, Y.-Q., Waqas, H., Al-Khaled, K., Farooq, U., Khan, S.U., Khan, M.I., Chu, Y.-M., Qayyum, S.: Bioconvection analysis for Sutterby nanofluid over an axially stretched cylinder with melting heat transfer and variable thermal features: a Marangoni and solutal model. Alex. Eng. J. 60(5), 4663–4675 (2021)
- Anjum, N., Khan, W.A., Ali, M., Hussain, I., Waqas, M., Irfan, M.: Thermal performance analysis of Sutterby nanoliquid subject to melting heat transportation. Int. J. Mod. Phys. B 37(19), 2350185 (2023)
- Venkatadri, K., Gaffar, S.A., Prasad, V.R., Khan, B.M.H., Anwar Bég, O.: Melting heat transfer analysis
 of electrically conducting nanofluid flow over an exponentially shrinking/stretching porous sheet with
 radiative heat flux under magnetic field. Heat Transf. 49, 4281–4303 (2020)
- Garvandha, M., Narla, V.K., Tripathi, D., Anwar Bég, O.: Modelling the impact of melting and nonlinear radiation on reactive buongiorno nanofluid boundary layer flow from an inclined stretching cylinder with cross-diffusion and curvature effects. In: Tripathi, D., Sharma, R.K. (eds.) Energy Systems and Nanotechnology. Advances in Sustainability Science and Technology. Springer, Singapore (2021). https:// doi.org/10.1007/978-981-16-1256-5_15
- Ali, U., Irfan, M., Akbar, N.S., Rehman, K.U., Shatanawi, W.: Dynamics of Soret–Dufour effects and thermal aspects of Joule heating in multiple slips Casson–Williamson nanofluid. Int. J. Mod. Phys. B (2023). https://doi.org/10.1142/S0217979224502060
- Irfan, M., Aftab, R., Khan, M.: Thermal performance of Joule heating in Oldroyd-B nanomaterials considering thermal-solutal convective conditions. Chin. J. Phys. 71, 444–457 (2021). https://doi.org/10.1016/j.cjph.2021.03.010
- Irfan, M., Anwar, M.S., Kebail, I., Khan, W.A.: Thermal study on the performance of Joule heating and Sour–Dufour influence on nonlinear mixed convection radiative flow of Carreau nanofluid. Tribol. Int. 188, 108789 (2023). https://doi.org/10.1016/j.triboint.2023.108789
- Ali, U., Irfan, M.: Thermal aspects of multiple slip and Joule heating in a Casson fluid with viscous dissipation and thermosolutal convective conditions. Int. J. Mod. Phys. B 37, 2350043 (2023). https://doi. org/10.1142/S0217979223500431



- Anusha, T., Mahabaleshwar, U.S., Hatami, M.: Navier slip effect on the thermal flow of Walter's liquid B
 flow due to porous stretching/shrinking with heat and mass transfer. Case Stud. Therm. Eng. 28, 101691
 (2021)
- Venkateswarlu, B., Narayana, P.V.S.: Cu-Al2O3/H2O hybrid nanofluid flow past a porous stretching sheet due to temperature-dependent viscosity and viscous dissipation. Heat Transf. 50, 432–449 (2021)
- Sharma, K.: FHD flow and heat transfer over a porous rotating disk accounting for Coriolis force along with viscous dissipation and thermal radiation. Heat Transf. 51, 4377–4392 (2022). https://doi.org/10. 1002/htj.22504
- Sharma, K., Vijay, N., Kumar, S., Makinde, O.D.: Hydromagnetic boundary layer flow with heat transfer past a rotating disc embedded in a porous medium. Heat Transf. 50, 4342–4353 (2021). https://doi.org/ 10.1002/htj.22078
- Amjad, M., Ahmed, I., Ahmed, K., Alqarni, M.S., Akbar, T., Muhammad, T.: Numerical solution of magnetized williamson nanofluid flow over an exponentially stretching permeable surface with temperature dependent viscosity and thermal conductivity. Nanomaterials 12, 3661 (2022). https://doi.org/10.3390/nano1220366
- Alhowaity, A., Bilal, M., Hamam, H., Alqarni, M.M., Mukdasai, K., Ali, A., et al.: Non-Fourier energy transmission in power-law hybrid nanofluid flow over a moving sheet. Sci. Rep. 12(1), 10406 (2022). https://doi.org/10.1038/s41598-022-14720-x
- Amjad, M., Ahmed, I., Ahmed, K., Alqarni, M.S., Akbar, T., Muhammad, T.: Numerical solution of magnetized williamson nanofluid flow over an exponentially stretching permeable surface with temperature dependent viscosity and thermal conductivity. Nanomaterials 12, 3661 (2022). https://doi.org/10.3390/nano12203661
- Mukhopadhyay, S., Gorla, R.S.R.: Effects of partial slip on boundary layer flow past a permeable exponential stretching sheet in presence of thermal radiation. Heat Mass Transf. 48, 1773–1781 (2012)

Publisher's Note Springer Nature remains neutral with regard to jurisdictional claims in published maps and institutional affiliations.

Springer Nature or its licensor (e.g. a society or other partner) holds exclusive rights to this article under a publishing agreement with the author(s) or other rightsholder(s); author self-archiving of the accepted manuscript version of this article is solely governed by the terms of such publishing agreement and applicable law.

